International Journal of Modern Physics E

STAR results on strangeness and electric charge dependent splitting of rapidity-odd directed flow

Ashik Ikbal Sheikh* (for the STAR Collaboration)
Department of Physics, Kent State University
Kent, OH 44242, USA
asheikh2@kent.edu
ashikhep@gmail.com

Rapidity-odd directed flow (v_1) of multi-strange baryons (Ξ and Ω) at mid-rapidity is reported for Au+Au collisions as recorded by the STAR detector at the Relativistic Heavy Ion Collider (RHIC). We focus on particle species where all constituent quarks are produced, such as $K^-(\bar{u}s)$, $\bar{p}(\bar{u}\bar{u}\bar{d})$, $\bar{\Lambda}(\bar{u}\bar{d}\bar{s})$, $\phi(s\bar{s})$, $\overline{\Xi}^+(\bar{d}\bar{s}\bar{s})$, $\Omega^-(sss)$ and $\overline{\Omega}^+(\bar{s}\bar{s}\bar{s})$, and demonstrate using a novel analysis method that the coalescence sum rule holds in a common kinematic region for hadron combinations with identical quark content. We examine the coalescence sum rule as a function of rapidity for non-identical quark content having the same quark-level mass but different strangeness (ΔS) and electric charge (Δq). The difference in the directed flow of different quark and anti-quark combinations, e.g., $v_1(\Omega^-(sss)) - v_1(\bar{\Omega}^+(\bar{s}\bar{s}\bar{s}))$, is a measure of coalescence sum rule violation, and we call it directed flow splitting (Δv_1). We measure ΔS and Δq dependence of the Δv_1 slope ($d\Delta v_1/dy$) between produced quarks and anti-quarks in Au+Au collisions at $\sqrt{s_{NN}} =$ 27 GeV and 200 GeV. Measurements have been compared with A Multi-Phase Transport (AMPT) and Parton-Hadron String Dynamics (PHSD) model with electromagnetic field calculations.

Keywords: Heavy-ion collisions; multi-strange; directed flow; electro-magnetic field.

PACS numbers:

1. Introduction

The azimuthal anisotropic flow of emitted particles is one of the most important and effective experimental observables for characterizing the matter formed in heavy-ion collisions.[1–3] The anisotropic flow can be expressed in terms of Fourier coefficients extracted from the azimuthal distribution of the final state particles. The first harmonic coefficient of the Fourier expansion relative to the reaction plane (Ψ_{RP}) is defined as rapidity-odd directed flow, v_1. Nuclear transport[4] and hydrodynamic[5] model calculations indicate that v_1 is sensitive to the early stages of the collisions.

*Speaker (10th International Conference on New Frontiers in Physics (ICNFP 2021), Kolymbari, Crete, Greece)

In high-energy collisions, strange quarks (s and $\bar{s}$) are produced through partonic interactions ($gg \rightarrow s\bar{s}$, $q\bar{q} \rightarrow s\bar{s}$) in an enhanced manner in the plasma phase and retain their identity during the hadronization phase which ensures the production of strange particles, such as K, Λ, $\bar{\Lambda}$, ϕ, Ξ and Ω, in the collisions.[6,7] Multi-strange baryons (Ξ and Ω) have low scattering cross section, and early thermal freeze-out time compared to non- or single-strange particles.[8] In other words, multi-strange particles are emitted almost directly from the phase boundary of the hadronizing fireball and hence they carry important information of the earlier stages of the collisions.[9] Since v_1 is sensitive to the early stages too, the measurements of v_1 of multi-strange baryons might be a good probe to study early collision dynamics. It has also been argued that an extremely strong magnetic field ($\vec{B}$) is produced in the early stages of non-central heavy-ion collisions due to the motion of the charged spectators that pass each other rather. The presence of an early-time magnetic field has important implications for the motion of the final-state charged particles that we measure in experiments.[10–12] As the charged spectators fly away, the produced $\vec{B}$ decays down quickly and generates an electric current in the plasma owing to the Faraday effect. The charged spectators can also exert an electric force on the charged constituents in the plasma due to Coulomb effect. Along with that, the plasma has a longitudinal expansion velocity along the beam direction and hence perpendicular to $\vec{B}$, and the Lorentz force pushes charged particles and anti-particles of the plasma in opposite directions, perpendicular to both the direction of the plasma's longitudinal velocity and $\vec{B}$. This is called the Hall effect. The combination of Faraday, Coulomb, and Hall effects greatly influence the v_1 of the different produced particles depending upon their charge,[10–12] which eventually leads to the splitting of v_1. Hence, the study of charge-dependent v_1 and the splitting are deserving of focused attention among theorists and experimentalists.

The splitting between opposite-charge hadron pairs like $\pi^{\pm}$, $K^{\pm}$, $p(\bar{p})$, etc., has been calculated in the literature.[10,13–15] The splitting between heavy (anti-)particle pairs ($D^0\,(c\bar{u}) - \bar{D}^0\,(\bar{c}u)$) has also been computed and found to be affected by the produced $\vec{B}$.[16] This is due to the fact that charm and anti-charm are produced early and get the strongest kicks from the early-time strong $\vec{B}$ field. From the experimental side, there are many measurements of v_1 for different particle species at RHIC [17–21] and the LHC.[22] STAR measured charge-dependent v_1 splitting between positively and negatively charged hadrons in Cu+Au and Au+Au collisions at $\sqrt{s_{NN}} = 200$ GeV.[23] Due to the larger Coulomb force in asymmetric Cu+Au collisions compared to the symmetric Au+Au case, a large v_1 splitting is observed in the Cu+Au system. ALICE measured v_1 splitting using inclusive charged hadrons in Pb+Pb collisions at $\sqrt{s_{NN}} = 2.76$ TeV.[22] Also, the v_1 splitting between D^0 and $\bar{D}^0$ mesons was reported by the STAR[24] and ALICE[22] collaborations in $\sqrt{s_{NN}} = 200$ GeV Au+Au and $\sqrt{s_{NN}} = 2.76$ TeV Pb+Pb collisions, respectively. Note that a stronger splitting between D^0 and $\bar{D}^0$ compared to the inclusive charged hadrons is seen at the LHC, however the splitting at STAR is consistent with zero within large uncertainties. The large splitting at the LHC is attributed to the effect of the early-stage strong $\vec{B}$.

In the STAR experiment, measurements of D^0 and $\bar{D^0}$ below $\sqrt{s_{NN}} = 200$ GeV are difficult due to the lower heavy flavour production rate and the absence of the Heavy Flavour Tracker (HFT) detector during Beam Energy Scan (BES) phase-II data taking. Charge-dependent v_1 splitting can be measured using light hadrons, since they are produced in abundance and there were suitable detectors installed during the BES-II run periods. However, there are difficulties in interpreting the splitting using light flavour, especially when the effects of electromagnetic fields are concerned. For example, among light hadrons, there are many (anti-)particles that contain u and d quarks, which can be either transported from beam rapidity[25] or produced in the collisions. The transported u and d quarks suffer a lot more interactions than the produced quarks before ending up in a measured hadron, and hence they have different v_1 from the produced quarks.[26] So, there is already a splitting due to the transport, which act as a background for the electromagnetic-field-driven splitting. Subtracting such contamination in experiment is very difficult. Our experimental analysis approach bypasses the transported quarks and avoids the contamination by choosing particles composed of produced constituent quarks only ($\bar{u}$, $\bar{d}$, s and $\bar{s}$). The details of the approach can be found in Ref.[27] and will also be discussed briefly in Section 2.2.

In these proceedings, we show the measurements of v_1 of multi-strange baryons (Ξ and Ω). We also present the v_1 splitting as a function of electric charge difference Δq and strangeness difference ΔS, using light hadrons from Au+Au collisions at $\sqrt{s_{NN}} = 27$ and 200 GeV. These proceedings are organized as follows: In the next section, we refer to the STAR experimental setup and the employed analysis approach. We discuss results in Sec. 3. Section 4 is devoted to a summary.

2. Experimental setup and the analysis approach

2.1. *STAR detector setup and analysis cuts*

The STAR detector[28] system is an excellent experimental setup for track reconstruction, vertexing, and particle identification at RHIC. The main tracking detector is located in a uniform magnetic field of maximum value 0.5 T, which provides charged particle momentum measurements. A large volume Time Projection Chamber (TPC),[29] covering a pseudo-rapidity range $|\eta| \leq 1$ is used for charged particle tracking, vertexing, and particle identification using ionization energy loss. Time-of-flight information from the TOF detector[30] is also used for particle identification. There are forward-rapidity detectors, namely the Event-Plane Detectors (EPDs) ($2.1 < |\eta| < 5.1$)[31] and Zero-Degree Calorimeter with Shower-Maximum Detectors (ZDC-SMDs) ($|\eta| > 6.3$),[32] that can measure event planes of the collisions.

The analysis reported here is carried out using high statistics data samples for Au+Au collisions at $\sqrt{s_{NN}} = 27$ GeV and 200 GeV, recorded by the STAR detector in the years 2018 and 2016, respectively. We restrict the primary vertex position of each event to be along the beam direction with $|V_z| < 40$ cm, and along the radial direction transverse to the beam axis with $V_r < 2$ cm at $\sqrt{s_{NN}} = 27$ GeV; and $|V_z| < 70$ cm, $V_r < 2$ cm at $\sqrt{s_{NN}} = 200$ GeV. The tracks are required to have $p_T > 0.2$ GeV/c and a distance of closest approach (DCA) from the primary vertex, DCA ≤ 3 cm. Additional requirements for track selection are: at least 15 space points in the TPC acceptance, and the ratio of the number of measured space points to the maximum possible number of space points should be greater than 0.52. Particles are identified using information from TPC and TOF detectors. Particle identification cuts applied are: $0.4 < p_T < 5$ GeV/c, $|n_\sigma| \leq 2$ for protons and anti-protons; $p_T > 0.2$ GeV/c, momentum < 1.6 GeV/c and $|n_\sigma| \leq 2$ for charged pions and kaons, where n_σ denotes standard deviation from the most probable dE/dx for that particle type. Systematic uncertainties on the measurements are obtained by varying these analysis cuts and removing the effects of statistical fluctuations, as prescribed by Barlow.[33]

We have reconstructed Λ, $\bar{\Lambda}$, Ξ^-, $\overline{\Xi}^+$, Ω^-, and $\overline{\Omega}^+$ within $0.2 < p_T < 5$ GeV/c using a Kalman filter (KF) method.[34,35] The KF-Particle package exploits the quality of the track fit as well as the decay topology. The decay channels used for the reconstruction are: $\Lambda(\bar{\Lambda}) \rightarrow p\pi^-(\bar{p}\pi^+)$, $\Xi^-(\overline{\Xi}^+) \rightarrow \Lambda\pi^-(\bar{\Lambda}\pi^+)$ and $\Omega^-(\overline{\Omega}^+) \rightarrow \Lambda K^-(\bar{\Lambda}K^+)$.[36] ϕ-mesons are reconstructed in K^+K^- channel using the invariant mass technique with pair rotation background subtraction.

2.2. *Analysis approach*

The analysis approach is based on the quark coalescence mechanism, where the anisotropic collective flow is assumed to be imparted before hadronization and the observed particles are assumed to form via coalescence of constituent quarks. This mechanism of particle formation implies a sum rule, called the coalescence-inspired sum rule,[21] and the number-of-constituent-quark (NCQ) scaling of the measured flow immediately follows from there. Directed flow of a suitably-chosen hadron species is consistent with the sum of the directed flow of its constituent quarks:

$$v_1(\text{hadron}) = \sum_i v_1(q_i), \tag{1}$$

where the sum runs over the v_1 for the two constituent quarks q_i in a meson and the three in a baryon. These constituent quarks can either be produced in the collisions or transported from the incoming nuclei. There are many particle species composed of constituent u and d quarks, which might or might not be transported from the incoming nuclei. The v_1 of the transported quarks (u and d) in general is quite different from that of produced quarks ($\bar{u}$, $\bar{d}$, s and $\bar{s}$). This in turn leads to a difference between v_1 of a particle containing u or d quarks that could be either produced or transported, and v_1 of another particle containing produced quarks only ($\bar{u}$, $\bar{d}$, s and $\bar{s}$). This fact greatly complicates[37] the interpretation of v_1 splitting between positive and negative hadrons in terms of possible electromagnetic field effects. In experiment, it is hard to distinguish transported and produced

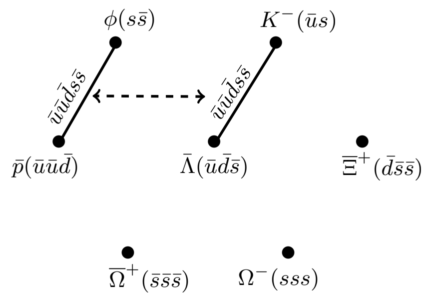

Fig. 1. Diagram[27] showing the seven produced particles composed of produced (non-transported) quarks only. We combine ϕ with $\bar{p}$ and K^- with $\bar{\Lambda}$ so that these two combinations have identical constituent quarks $\bar{u}\bar{u}\bar{d}s\bar{s}$ that correspond to the same mass at the constituent level $\Delta m = 0$, the same strangeness $\Delta S = 0$ and the same electric charge $\Delta q = 0$. The measured directed flow of these two combinations must be similar if the coalescence sum rule holds. The geometric arrangement of the seven hadron species has no special significance and is chosen simply to facilitate illustration of the chosen combinations.

quarks and hence, here we study those particles which contain produced quarks only, namely, $K^-(\bar{u}s)$, $\bar{p}(\bar{u}\bar{u}\bar{d})$, $\bar{\Lambda}(\bar{u}\bar{d}\bar{s})$, $\phi(s\bar{s})$, $\overline{\Xi}^+(\bar{d}\bar{s}\bar{s})$, $\Omega^-(sss)$, and $\overline{\Omega}^+(\bar{s}\bar{s}\bar{s})$.

Index	Quark mass	Charge	Strangeness	Δv_1 combination
1	$\Delta m = 0$	$\Delta q = 0$	$\Delta S = 0$	$[\bar{p}(\bar{u}\bar{u}\bar{d}) + \phi(s\bar{s})] - [K^-(\bar{u}s) + \bar{\Lambda}(\bar{u}\bar{d}\bar{s})]$
2	$\Delta m \approx 0$	$\Delta q = \frac{2}{3}$	$\Delta S = 1$	$[\bar{\Lambda}(\bar{u}\bar{d}\bar{s})] - [\frac{1}{2}\phi(s\bar{s}) + \frac{2}{3}\bar{p}(\bar{u}\bar{u}\bar{d})]$
3	$\Delta m \approx 0$	$\Delta q = 1$	$\Delta S = 2$	$[\bar{\Lambda}(\bar{u}\bar{d}\bar{s})] - [\frac{1}{3}\Omega^-(sss) + \frac{2}{3}\bar{p}(\bar{u}\bar{u}\bar{d})]$
4	$\Delta m \approx 0$	$\Delta q = \frac{4}{3}$	$\Delta S = 2$	$[\bar{\Lambda}(\bar{u}\bar{d}\bar{s})] - [K^-(\bar{u}s) + \frac{1}{3}\bar{p}(\bar{u}\bar{u}\bar{d})]$
5	$\Delta m \approx 0$	$\Delta q = \frac{4}{3}$	$\Delta S = 2$	$[\overline{\Xi}^+(\bar{d}\bar{s}\bar{s})] - [\phi(s\bar{s}) + \frac{1}{3}\bar{p}(\bar{u}\bar{u}\bar{d})]$
6	$\Delta m = 0$	$\Delta q = 2$	$\Delta S = 6$	$[\overline{\Omega}^+(\bar{s}\bar{s}\bar{s})] - [\Omega^-(sss)]$
7	$\Delta m \approx 0$	$\Delta q = \frac{7}{3}$	$\Delta S = 4$	$[\overline{\Xi}^+(\bar{d}\bar{s}\bar{s})] - [K^-(\bar{u}s) + \frac{1}{3}\Omega^-(sss)]$

Table 1. This table shows differences between combinations formed from seven particle species composed of produced quarks only. For every combination, the constituent quark mass difference (Δm) is zero or near-zero, while the charge difference (Δq) and strangeness difference (ΔS) are varied as tabulated. Index 1 is illustrated in diagrammatic form in Fig. 1.

The above seven particles have different flavour, electric charge (q) and mass (m). The v_1 is sensitive to quark flavour and mass. How do we compare the v_1 of these different particles and search for possible EM-field-driven splitting? Firstly, we choose a common kinematic region, p_T/n_q–y (where n_q is the number of constituent quarks in the particle and y is the rapidity of the particle) for all seven particle species and test the coalescence sum rule (Eq. (1)) by combining the different particles so that the combinations have identical quark content. In other words, we measure v_1 of the individual particle and test the following in the selected kinematic region,

$$v_1[\bar{p}(\bar{u}\bar{u}\bar{d})] + v_1[\phi(s\bar{s})] = v_1[K^-(\bar{u}s)] + v_1[\bar{\Lambda}(\bar{u}\bar{d}\bar{s})]. \tag{2}$$

In Eq. (2), both left and right sides have the identical constituent quark content of $\bar{u}\bar{u}\bar{d}s\bar{s}$. However, the quarks are shared differently within the two pairs of hadrons. This is illustrated in Fig. 1 (taken from Ref.[27]).

Secondly, after verifying that Eq. (2) holds within measured uncertainties in the selected kinematic region, we move on and form combinations among the seven particles in such a way that the combinations have the same or similar mass at the constituent quark level ($\Delta m \approx 0$), but non-zero electric charge difference Δq and non-zero strangeness difference ΔS. The difference Δv_1 of such combinations ($\Delta m \approx 0$), is called "splitting of v_1" and the slope of the Δv_1 is a measure of the splitting. For example, Eq. (2) can be expressed in terms of Δv_1 as follows:

$$\Delta v_1(\Delta q = 0,\, \Delta S = 0) = \{v_1[\bar{p}(\bar{u}\bar{u}\bar{d})] + v_1[\phi(s\bar{s})]\} - \{v_1[K^-(\bar{u}s)] + v_1[\bar{\Lambda}(\bar{u}\bar{d}\bar{s})]\}. \tag{3}$$

We obtain different combinations as shown in Table 1 where index 1 is the identical quark combination case ($\Delta q = 0$ and $\Delta S = 0$) (Eq. (2)) and indices 2-7 are non-identical quark combination cases ($\Delta q \neq 0$ and $\Delta S \neq 0$). In the combinations, we assume that masses of u and d are the same, and different from s and $\bar{s}$ quarks, i.e., $m_u \sim m_d \neq m_s (= m_{\bar{s}})$. Two degenerate combinations, indices 4 and 5, have the same $\Delta q = 4/3$ and $\Delta S = 2$. There are other possible combinations similar to the ones listed in Table 1. Measuring the Δv_1 of all the combinations in Table 1 enables us to measure the splitting with different Δq and ΔS. Of course, the increase in Δq in Table 1 is also associated with a change in ΔS. This is an unavoidable consequence of the quantum numbers carried by the constituent quarks.

3. Results and discussion

Figure 2 shows invariant mass distributions of Λ-π pairs (left plot) and Λ-K pairs (right plot) for 20%-80% centrality in Au+Au collisions at $\sqrt{s_{NN}} = 27$ GeV.

We employed the event plane method to measure v_1 of each particle:

$$v_1 = \langle \cos(\phi - \Psi_1) \rangle / \mathrm{Res}\{\Psi_1\}, \tag{4}$$

where ϕ is the track azimuthal angle measured in the TPC and $\mathrm{Res}\{\Psi_1\}$ is the event plane resolution with Ψ_1 being the event plane angle, estimated from EPDs or ZDC-SMDs. In Fig. 3, we display the first measurements of Ξ and Ω baryon v_1 for 10%-40% centrality in Au+Au collisions at $\sqrt{s_{NN}} = 27$ and 200 GeV. We perform a fit to the results with a linear function, $v_1(y) = Cy$, where C being the fitting parameter, and y being the rapidity. We found, $C = -0.021 \pm 0.008$ (-0.006 ± 0.01) for Ω^- ($\overline{\Omega}^+$) and $C = -0.009 \pm 0.002$ (-0.015 ± 0.003) for Ξ^- ($\overline{\Xi}^+$) at $\sqrt{s_{NN}} = 27$ GeV. For $\sqrt{s_{NN}} = 200$ GeV, $C = -0.003 \pm 0.006$ (-0.003 ± 0.005) for Ω^- ($\overline{\Omega}^+$)

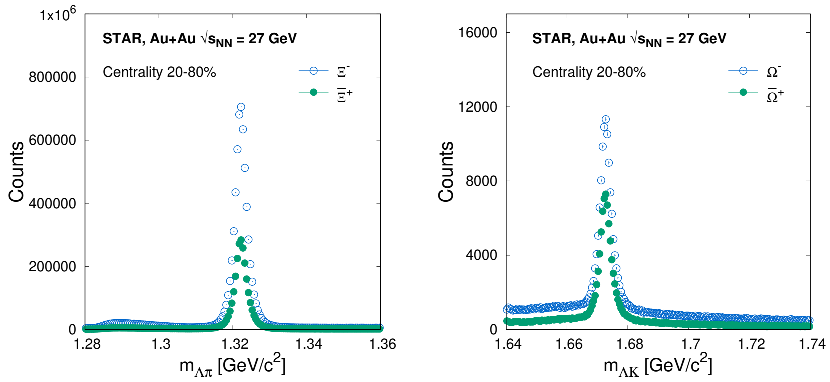

Fig. 2. Invariant mass distributions of Λ-π (left) and Λ-K (right) pairs for 20%-80% centrality in Au+Au collisions at $\sqrt{s_{NN}} = 27$ GeV.

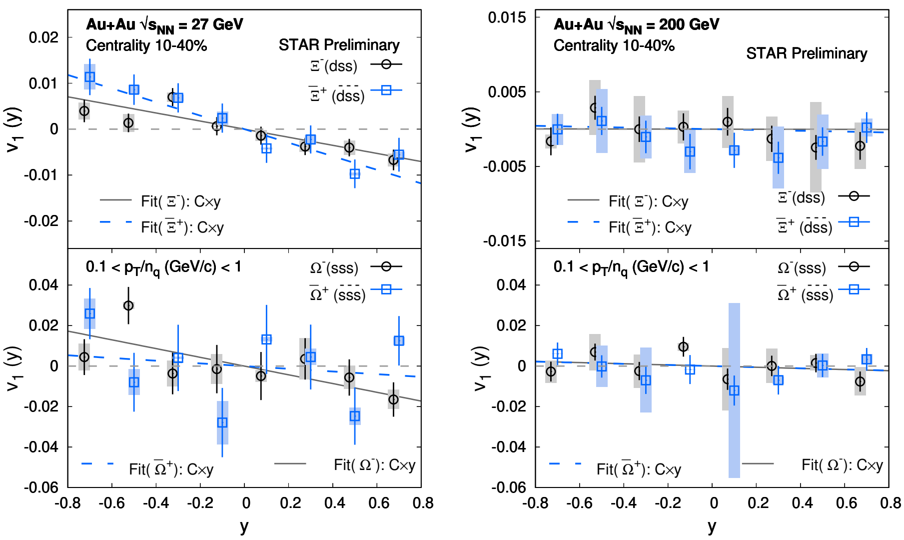

Fig. 3. Directed flow (v_1) of Ξ^-, $\overline{\Xi}^+$, Ω^- and $\overline{\Omega}^+$ as a function of rapidity (y) for 10%-40% centrality in Au+Au collisions at $\sqrt{s_{NN}} = 27$ and 200 GeV.

and $C = -0.000 \pm 0.002$ (-0.0005 ± 0.002) for Ξ^- $(\overline{\Xi}^+)$. Note that the slopes at $\sqrt{s_{NN}} = 200$ GeV have large errors. There is a hint of a larger v_1 for Ω^- compared to Ξ baryons at $\sqrt{s_{NN}} = 27$ GeV, but statistical uncertainties are also large here.

We also measure v_1 of the other produced particle species (K^-, $\bar{p}$, $\bar{\Lambda}$, and ϕ) and calculate Δv_1 for all seven combinations as shown in Table 1. Figure 4 displays the measured $\Delta v_1(y)$ for $\Delta q =0$, 2/3, 4/3 and $\Delta S =0$, 1, 2 in 10%-40% central Au+Au

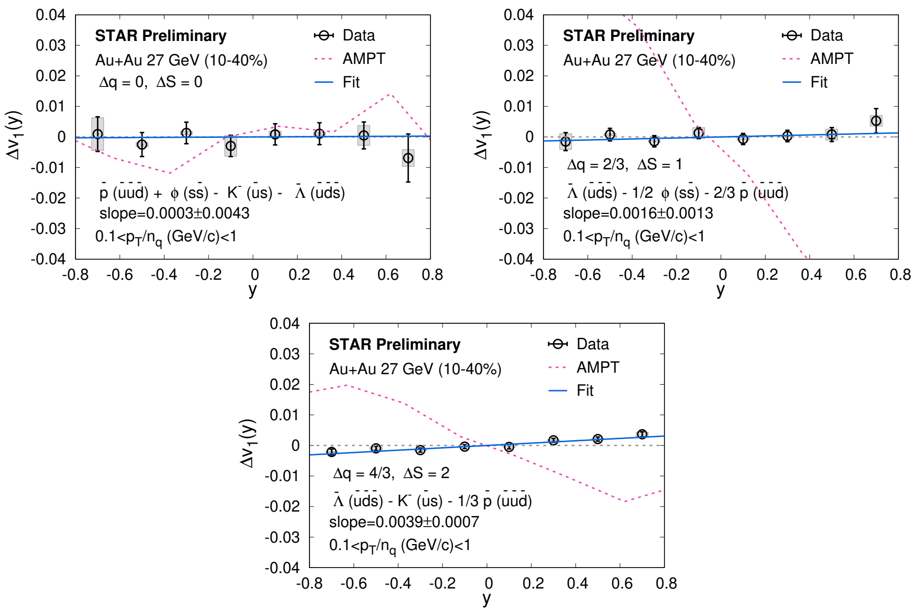

Fig. 4. Δv_1 as a function of rapidity (y) for Δq =0, 2/3, 4/3 and ΔS =0, 1, 2 in 10%-40% central Au+Au collisions at $\sqrt{s_{NN}}$ = 27 GeV. AMPT model calculations[39] are compared with the measurements.

collisions at $\sqrt{s_{NN}} = 27$ GeV. The measurements are fitted with a linear function and the slope parameter is extracted. For $\Delta q = 0$ and $\Delta S = 0$ (identical quark combination case), the value of the slope is a minimum compared to $\Delta q = 2/3$ and 4/3 and $\Delta S = 1$ and 2 cases. This minimum deviation from zero indicates that the coalescence sum rule holds with the identical quark combination as mentioned above in Eqs. (2) and (3). The slope deviates more from zero as we move to $\Delta q = 2/3$ and 4/3 and $\Delta S = 1$ and 2. This deviation is presumably caused by the non-zero Δq and ΔS.

A Multi-Phase Transport (AMPT)[38] model calculations are compared with the measured Δv_1. We took the AMPT results for individual particle v_1 from Ref.[39] and calculated the Δv_1 for different Δq and ΔS. It seems that the model calculations can describe the measured Δv_1 for the $\Delta q = 0$, $\Delta S = 0$ case, although the calculations show unexpected fluctuations around zero. For $\Delta q = 2/3$ and 4/3 and $\Delta S = 1$ and 2, AMPT shows a completely opposite trend compared to the data.

Figure 5 depicts the Δv_1-slope ($d\Delta v_1/dy$) at mid-rapidity as a function of Δq and ΔS for 10%-40% centrality in Au+Au collisions at $\sqrt{s_{NN}}$ = 27 GeV and $\sqrt{s_{NN}}$ = 200 GeV. Note that there are two data points at $\Delta q = 4/3$ and $\Delta S =$ 2 for each collision energy. These two points are the degenerate points (index 4 and 5 in Table 1), plotted here to show the consistency between them. We fit the measurements at both collision energies with a linear function and show the

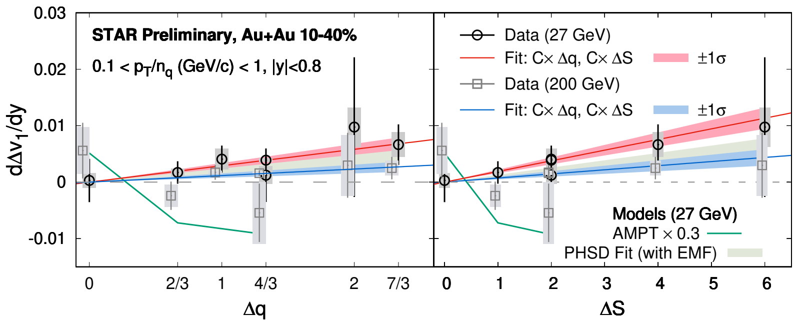

Fig. 5. Left panel: Δv_1 slope ($d\Delta v_1/dy$) at mid-rapidity as a function of electric charge difference (Δq, see Table 1) for 10%-40% centrality in Au+Au collisions at $\sqrt{s_{NN}} = 27$ GeV and $\sqrt{s_{NN}} = 200$ GeV. AMPT and PHSD+EM field model calculations are also plotted here.
Right panel: The same as the left panel, but as a function of strangeness (ΔS, see Table 1). Note that the data points for $\sqrt{s_{NN}} = 200$ GeV in both panels are staggered horizontally for better visualization.

one-σ band of the fits around each fitted line. The red and blue lines are the fits to the $\sqrt{s_{NN}} = 27$ and 200 GeV data points, respectively. We observe when $\Delta q = 0$ and $\Delta S = 0$, the $d\Delta v_1/dy$ is close to zero within uncertainties. The identical quark combination (index 1 of Table 1) leads to $\Delta q = 0$ and $\Delta S = 0$ which seems to be the best scenario to verify the coalescence-inspired sum rule. For non-identical quark combinations ($\Delta q \neq 0$ and $\Delta S \neq 0$), the $d\Delta v_1/dy$ seems to deviate from zero and reaches a maximum when Δq and ΔS are a maximum. In other words, there is an increasing trend of $d\Delta v_1/dy$ with Δq and ΔS. The strength of the Δv_1 slope is stronger at $\sqrt{s_{NN}} = 27$ GeV than at $\sqrt{s_{NN}} = 200$ GeV. The AMPT and Parton-Hadron String Dynamics (PHSD)+electromagnetic field (EMF) model[40,41] calculations have also been compared here with the data. The AMPT model predictions at $\sqrt{s_{NN}} = 27$ GeV are displayed by the green line, and they do not agree with the measurements. The PHSD+EMF calculations are shown by the light green band, and the calculations can explain the data within uncertainties. The PHSD model with EMF assumes that all electric charges are affected by the strong EMF and this results in a splitting of v_1 between positive and negative particles as observed in Fig 5. This splitting increases as the electric charge difference between positive and negative particles increases.

4. Summary

In summary, we report the first measurements of directed flow, $v_1(y)$, of multi-strange baryons (Ξ and Ω) in Au+Au collisions at $\sqrt{s_{NN}} = 27$ GeV and 200 GeV. We find that there is a hint of a relatively larger v_1-slope for Ω^- compared to the Ξ baryons, however the statistical significance of the difference is 2.68σ. We focus on the produced particle species (K^-, $\bar{p}$, $\bar{\Lambda}$, ϕ, $\overline{\Xi}^-$, Ω^-, and $\overline{\Omega}^+$), and test the coalescence sum rule by using a novel analysis technique. Then we measure directed flow splitting as a function of Δq and ΔS. The Δv_1 slope $d\Delta v_1/dy$, a measure of splitting, increases with Δq and ΔS. The strength of the splitting increases going from $\sqrt{s_{NN}}$ = 200 GeV to $\sqrt{s_{NN}}$ = 27 GeV. The observed $d\Delta v_1/dy$ is compared with AMPT and PHSD model calculations. AMPT model predictions do not agree with the measurements. Measurements are consistent with the PHSD model calculations that include the effect of the electromagnetic field.

Acknowledgments

Author acknowledges support from the Office of Nuclear Physics within the US DOE Office of Science, under Grant DE-FG02-89ER40531.

References

1. J.-Y. Ollitrault, *Phys. Rev. D* **46**, 229 (1992).
2. S. Voloshin, and Y. Zhang, *Z. Phys. C.* **70**, 665 (1996).
3. A. M. Poskanzer, and S. A. Voloshin, *Phys. Rev. C* **58**, 1671 (1998).
4. S. A. Bass *et al.*, *Prog. Part. Nucl. Phys.* **41**, 255 (1998).
5. U. W. Heinz, Landolt-Bornstein, **23**, 240 (2010).
6. J. Rafelski, and B. Muller, *Phys. Rev. Lett.* **48**, 1066 (1982); [Erratum: *Phys. Rev. Lett.* **56**, 2334 (1986)].
7. A. Shor, *Phys. Rev. Lett.* **54**, 1122 (1985).
8. H. van Hecke, H. Sorge, and N. Xu, *Phys. Rev. Lett.* **81**, 5764 (1998).
9. J. Adams *et al.* (STAR Collaboration), *Phys. Rev. Lett.* **92**, 182301 (2004).
10. U. Gursoy, D. Kharzeev, E. Marcus, K. Rajagopal, and C. Shen, *Phys. Rev. C* **98**, 055201 (2018).
11. U. Gursoy, D. Kharzeev, K. Rajagop, *Phys. Rev. C* **89**, 054905 (2014).
12. A. Dubla, U. Gursoy, and R. Snellings *Mod. Phys. Lett. A* **35**, 2050324 (2020).
13. V. Voronyuk, V. D. Toneev, S. A. Voloshin, and W. Cassing, *Phys. Rev. C* **90**, 064903 (2014).
14. V. D. Toneev, V. Voronyuk, E. E. Kolomeitsev, and W. Cassing, *Phys. Rev. C* **95**, 034911 (2017).
15. L. Oliva, P. Moreau, V. Voronyuk, and E. Bratkovskaya, *Phys. Rev. C* **101**, 014917 (2020).
16. S. K. Das, S. Plumari, S. Chatterjee, J. Alam, F. Scar-dina, and V. Greco, *Phys. Lett. B* **768**, 260 (2017).
17. J. Adams *et al.* (STAR Collaboration), *Phys. Rev. C* **73**, 034903 (2006).
18. B. I. Abelev *et al.* (STAR Collaboration), *Phys. Rev. Lett.* **101**, 252301 (2008).
19. L. Adamczyk *et al.* (STAR Collaboration), *Phys. Rev. Lett.* **108**, 202301 (2012).
20. L. Adamczyk *et al.* (STAR Collaboration), *Phys. Rev. Lett.* **112**, 162301 (2014).
21. L. Adamczyk *et al.* (STAR Collaboration), *Phys. Rev. Lett.* **120**, 062301 (2018).
22. S. Acharya et al. (ALICE Collaboration), *Phys. Rev. Lett.* **125**, 022301 (2020).
23. L. Adamczyk *et al.* (STAR Collaboration), *Phys. Rev. Lett.* **118**, 012301 (2017).
24. J. Adam *et al.* (STAR Collaboration), *Phys. Rev. Lett.* **123**, 162301 (2019).
25. J. C. Dunlop, M. A. Lisa, and P. Sorensen, *Phys. Rev. C* **84**, 044914 (2011).
26. Y. Guo, F. Liu, and A. Tang, *Phys. Rev. C* **86**, 044901 (2012).
27. A. I. Sheikh, D. Keane, and P. Tribedy, *Phys. Rev. C* **105**, 014912 (2022).
28. K. H. Ackermann *et al.* (STAR Collaboration), *Nucl. Instrum. Meth. A* **499**, 624 (2003).

29. M. Anderson *et al.*, *Nucl. Instrum. Meth. A* **499**, 659 (2003).
30. B. Bonner *et al.*, *Nucl. Instrum. Meth. A* **508**, 181 (2003).
31. J. Adams *et al.*, *Nucl. Instrum. Meth. A* **968**, 163970 (2020).
32. L. Adamczyk *et al.*, (STAR Collaboration), *Phys. Rev. Lett.* **108**, 202301 (2012).
33. R. Barlow, in *Conference on Advanced Statistical Techniques in Particle Physics(2002)*, hep-ex/0207026.
34. S. Gorbunov, *On-line reconstruction algorithms for the CBM and ALICE experiments*, Ph.D. thesis, Johann Wolfgang Goethe-Universitat (2013).
35. I. Kisel (CBM Collaboration), *J. Phys. Conf. Ser.* **1070**, 012015 (2018).
36. K. A. Olive *et al.*, *Chin. Phys. C* **38**, 090001 (2014).
37. G. Wang (STAR Collaboration), *Nucl. Phys. A* **982**, 415 (2019).
38. Z.-W. Lin, C. M. Ko, B.-A. Li, B. Zhang, and S. Pal, *Phys. Rev. C* **72**, 064901 (2005).
39. K. Nayak, S. Shi, N. Xu, and Z.-W. Lin, *Phys. Rev. C* **100**, 054903 (2019).
40. W. Cassing, and E. L. Bratkovskaya, *Phys. Rev. C* **78**, 034919 (2008).
41. V. Voronyuk *et al.*, *Phys. Rev. C* **83**, 054911 (2011).